Hydrol. Earth Syst. Sci. Discuss., 8, 4721–4752, 2011
www.hydrol-earth-syst-sci-discuss.net/8/4721/2011/
doi:10.5194/hessd-8-4721-2011


Hydrology and Earth System Sciences Discussions



# Diffuse hydrological mass transport through catchments: scenario analysis of physical and biogeochemical uncertainty effects

**K. Persson, J. Jarsjö, and G. Destouni**

Department of Physical Geography and Quaternary Geology, Stockholm University, 106 91, Stockholm, Sweden

Received: 8 April 2011 – Accepted: 15 April 2011 – Published: 12 May 2011

Correspondence to: K. Persson (klas.persson@natgeo.su.se)

Published by Copernicus Publications on behalf of the European Geosciences Union.





**Abstract**

This paper develops and investigates the applicability of a scenario analysis approach to quantify and map the effects of physical and biogeochemical variability, cross-correlation and uncertainty on expected hydrological mass loading from diffuse sources. The approach enables identification of conservative assumptions, uncertainty ranges, as well as pollutant/nutrient release locations and situations for which further investigations are most needed in order to reduce the most important uncertainty effects. The present scenario results provide different statistical and geographic distributions of advective travel times for diffuse hydrological mass transport, and show that neglect or underestimation of the physical advection variability implies substantial risk to underestimate pollutant and nutrient loads to downstream surface and coastal waters. This is particularly true for relatively high catchment-characteristic product between average attenuation rate and average advective travel time, for which mass delivery would be near zero under assumed transport homogeneity but can be orders of magnitude higher for variable transport conditions. A scenario of high advection variability, combined with a relevant average biogeochemical mass attenuation rate, emerges consistently from the example catchment results as a generally reasonable, conservative assumption for estimating maximum diffuse mass loading when the prevailing physical and biogeochemical variability and cross-correlation are uncertain. The geographic mapping of advective travel times for this high-variability scenario identifies also directly the potential hotspot areas with large mass loading to downstream surface and coastal waters, as well as their opposite, the potential lowest-impact areas within the catchment.

## 1 Introduction

Model estimations of diffuse hydrological mass transport are critical for biogeochemical cycle understanding, and successful and efficient environmental management. In many hydrological catchments with human activities, there are, apart from direct nutrient and pollutant discharges into surface waters, typically also diffuse sources at the land surface and below it, in soil, in mobile and immobile groundwater, and in sediments. Pollutants and excess nutrients that are transported from diffuse sources through the subsurface water system may yield considerable long-term loading to downstream surface and coastal waters (Malmström et al., 2004; Lindgren et al., 2007; Darracq et al., 2008; Olli and Destouni, 2008; Baresel and Destouni, 2009; Destouni et al., 2010; Basu et al., 2010). Catchment-scale water quality modelling and prediction must account for this subsurface transport, even if the main focus is on surface water quality.

However, all models of solute transport through subsurface and surface water subsystems, and whole catchments are inevitably associated with uncertainties. Over the last decades, many successive publications have investigated and quantified different types of uncertainty, and their implications for how to interpret hydrological mass transport models and their results, how to determine model applicability limits, and how to model, monitor and manage water pollution and its possible effects on health and environment (e.g., Dagan, 1989; Rubin, 1991, 2003; Cvetkovic et al., 1992; Destouni, 1992, 1993; Oreskes et al., 1994; Andricevic and Cvetkovic, 1996; Destouni and Graham, 1997; Batchelor et al., 1998; Graham et al., 1998; Jakeman et al., 1999; Eggleston and Rojstaczer, 2000; Gupta and Cvetkovic, 2000, 2002; Gren et al., 2000, 2002; Beven, 2001; Jarsjö et al., 2005; Botter et al., 2005, 2006, 2010; Baresel et al., 2006; Prieto et al., 2006; Refsgaard et al., 2006; Rinaldo et al., 2006; Baresel and Destouni, 2007; Jarsjö and Bayer-Raich, 2008; Persson and Destouni, 2009).

Different types of uncertainty in model interpretations and projections of waterborne mass transport can be structured and summarised in terms of the uncertainty dependencies and components along and across different observed/monitored and unobserved/unmonitored parts of the hydrological source-pathway-recipient continuum, including: (i) the spatiotemporal variability and historic-to-future development of driving forces and conditions, such as weather, climate, evapotranspiration and related land cover/use conditions, and human decisions, activities and pressures, which can create,



activate or deactivate nutrient/pollutant/tracer sources and/or decrease/increase their releases (e.g., Darracq et al., 2005; Prieto et al., 2006; Hagemann and Jacob, 2007; Jacob et al., 2007; Lindgren et al., 2007; Darracq et al., 2008; Jarsjö et al., 2008; Kyselý and Beranová, 2009; Destouni and Darracq, 2009; Bring and Destouni, 2011), (ii) the prevailing spatiotemporal configuration of actual source releases of mass at and below the land surface, in terms of source location, extent, release magnitude, and initial conditions of these at any point in time (e.g. Cvetkovic et al., 1992; Destouni, 1992, 1993; Baresel et al., 2006; Lindgren et al., 2007; Darracq et al., 2008; Edwards and Withers, 2008; Baresel and Destouni, 2009; Persson and Destouni, 2009; Bergknut et al., 2010), (iii) the physical flow and transport pathways, and associated physical water flow and mass transport velocities and travel times along these pathways from the sources to downstream observation points and receiving water environments (e.g. Destouni et al., 2001; McGuire et al., 2005; Destouni et al., 2008a; Grabs et al., 2009; Persson and Destouni, 2009; Beven, 2010; Darracq et al., 2010a, b; McDonnell et al., 2010), (iv) the spatiotemporal variability and cross-correlation of different physical and biogeochemical conditions that affect mass transport along the different flow and transport pathways (e.g. Cvetkovic and Shapiro, 1990; Destouni and Cvetkovic, 1991; Miralles-Wilhelm and Gelhar, 1996; Eriksson and Destouni, 1997; Jarsjö et al., 1997; Chang et al., 1999; Malmström et al., 2000, 2004, 2008; Cunningham and Fadel, 2007; Jardin, 2008), (v) the choice of mass transport measurement methods, the measurement errors, and the spatiotemporal coverage gaps implied by measured data only being available at some, chosen points of observation/monitoring (e.g., Destouni and Graham, 1997; Graham et al., 1998; Hannerz and Destouni, 2006; Beven, 2006; Jarsjö and Bayer-Raich, 2008; Bring and Destouni, 2009, 2011), and (vi) the subjectivity of chosen model representations (or possible total neglect) of potentially important contributing processes and/or geographic areas for which mass transport observation data are largely lacking (e.g., Lindgren and Destouni, 2004; Darracq and Destouni, 2005, 2007; Refsgaard et al., 2006; Destouni et al., 2006, 2008b, 2010; Ganoulis, 2009; Prieto and Destouni, 2011).

Among all these different types, components and dependencies of hydrological mass transport uncertainty, only some can be accounted for by realistic probability assignment and statistical quantification. However, also the remaining, statistically unquantifiable uncertainties need to be accounted for in some way. One way to achieve this is to consider scenarios that capture and bound different possible processes, system characteristics and future developments (e.g., Constanza, 2000; Molénat and Gascuel-Odoux, 2002; Swart et al., 2004; Arheimer et al., 2005; Jöborn et al., 2005; Popper et al., 2005; Refsgaard et al., 2006; de Vries, 2007; Macleod et al., 2007; Young et al., 2007; Lindgren et al., 2007; Darracq et al., 2008).

Recent studies have further combined probabilistic and scenario accounts of hydrological mass transport uncertainty, and discussed the needs and result implications of such combined approaches for rational guidance of management and abatement of water pollution (Baresel and Destouni, 2007; Persson and Destouni, 2009). These studies specifically addressed water pollution from local sources, with relatively limited and to large degree known source locations and extents (commonly referred to as point sources), for which bounding scenarios of different possible mass transport statistics could be relatively well defined and quantified. However, for pollutant/nutrient/tracer transport from diffuse sources, with continuous or patch-wise (e.g., from multiple, essentially unknown local/point sources) spatial distributions over more or less the whole landscape within a catchment area, such statistics are considerably more difficult to obtain (e.g., McDonnell et al., 2010; Darracq et al., 2010a, b).

In this paper we use and develop a scenario analysis approach to quantify some relevant statistical uncertainty bounds for hydrological mass transport from spatially widespread sources at and below the land surface, through soil and groundwater, to surface and coastal waters within and downstream of a catchment. We formulate and combine different scenarios of variability in physical and biogeochemical mass transport processes at the catchment scale, and quantify and map the scenario-associated transport and delivery of, for instance, tracer, pollutant or excess nutrient mass, from a diffuse source over the entire land area of a catchment to downstream surface or





coastal water recipients. We further assess the possible convergence, as well as the divergence and uncertainty among the different scenario results. The well-characterised Forsmark catchment in Sweden (e.g. Johansson et al., 2005; SKB, 2005; Werner et al., 2007; Jarsjö et al., 2008; Destouni et al., 2008a, 2010; Darracq et al., 2010a, b) is used as a specific case study example for this quantification, mapping and uncertainty assessment.

Uncertainty in physical and biogeochemical mass transport processes is often related to the spatial and temporal variability of the subsurface water system (soil, groundwater, sediments). In this study, we consider two different scenarios of physical subsurface variability, as implied by two quite opposite assumptions of the saturated hydraulic conductivity, $K$, distribution that may be encountered by the main pathways of diffuse subsurface flow and transport through the catchment. The physical (advective) transport process through these pathways is then represented by the advective solute travel time distributions that result from the two different $K$ variability scenarios. Previous calculations of travel time distributions in the Forsmark catchment example have considered a scenario of essentially constant $K$, prevailing along relatively high-conductive, preferential transport pathways through the catchment (Darracq et al., 2010a, b; Destouni et al., 2010). These calculations are here extended for a second, quite opposite flow and transport scenario, considering both spatial variability and statistical non-stationary in the transport-encountered $K$. This scenario represents a transport situation, where the flow and transport pathways go through and encounter the full $K$ variability that prevails within a catchment, instead of predominantly following preferential pathways of similar, relatively high $K$, as assumed in the first scenario.

In addition to and combined with the different scenarios of physical $K$ heterogeneity and resulting advective travel time distributions, we consider here also different scenarios with regard to the variability and cross-correlation with $K$ of the biogeochemical rate of pollutant/nutrient mass attenuation (decay or immobilisation by physical, chemical or biological processes) occurring along the physical transport pathways. Natural attenuation depends on subsurface characteristics, such as water flow velocity and mineralogy, which are also directly or indirectly related to hydraulic conductivity (Cunningham and Fadel, 2007; Jardine, 2008). With regard to bacterial degradation of organic contaminants, for instance, the subsurface permeability affects the availability of rate-limiting electron acceptors and donors, as well as the bacterial transport and community structure. Microbial processes can in turn also influence the permeability (Chapell, 2000). However, although there may clearly be a relation between attenuation and permeability, it is highly uncertain how and how strongly attenuation rates are correlated with $K$. Not even the sign of correlation can be determined a priori. The scientific literature contains empirical evidence and theoretical arguments for both negative and positive correlation (Cvetkovic and Shapiro, 1990; Destouni and Cvetkovic, 1991; Cozzarelli et al., 1999; Cunningham and Fadel, 2007; Jardine, 2008). A main objective of the present study is therefore to investigate how, and how much the hydrological mass transport from a catchment is affected by the complexity and uncertainty associated with the different possible scenarios of variability and cross-correlation of physical and biogeochemical mass transport processes among and along the transport pathways from diffuse sources to downstream surface and coastal waters.

## 2 Materials and methods

### 2.1 The Forsmark catchment example

Forsmark is a sparsely populated, 29.5 $km^2$ catchment of a Baltic Sea coastal stretch, located about 100 km north of Stockholm, Sweden. The prevailing hydrological conditions in this catchment have been extensively investigated, using measured and modelled geographical and hydrological data available at 10 m resolution (e.g. Johansson et al., 2005; SKB, 2005; Werner et al., 2007; Jarsjö et al., 2008; Destouni et al., 2008a, 2010; Darracq et al., 2010a, b).

The terrain in Forsmark is mildly undulating. Elevations range from 0 to 50 m a.s.l. (Brydsten and Strömgren, 2004). Quaternary deposits, predominantly till, cover the



gneiss and granite bedrock in most of the area. The depth to the groundwater table is mostly less than 1 m, and there is a strong correlation between small-scale topography and groundwater level. The undulating landscape appears to generate various small recharge areas of local groundwater flow systems (Werner et al., 2007). The long-term mean annual precipitation has been roughly estimated to be around 560 mm, of which about 25–30 % falls in the form of snow (Johansson and Öhman, 2008). Infiltration excess overland flow may occur, but only over short distances (SKB, 2008).

The landscape is characterised by forest, some small agricultural areas and a large number of lakes and wetlands. None of the lakes and wetlands is larger than 1 $km^2$, many are smaller than a hectare, but altogether they constitute 19 % of the total catchment area. Some of these lakes and wetlands are connected to each other and to the Baltic Sea by small streams. Others do not have any outlet and thus no surface water connection to the sea. About 10 % of the area drains to stretches of the coast with no surface water outlet. Measurements of stream discharge are available from four gauging stations, but the time series are too short to provide reliable information about the spatial variation of runoff in the area (Johansson and Öhman, 2008).

### 2.2 Quantification of advective solute travel times for physical heterogeneity scenarios

We quantified groundwater travel times in the Forsmark catchment for two different, quite opposite scenarios of how the saturated hydraulic conductivity $K$ may vary among and along the different pathways of diffuse solute transport in this example catchment area. In Fig. 1 the scenarios are schematically illustrated, and their respective $K$ distributions are shown. In scenario 1 the transport-encountered $K$ is essentially constant, representing transport that largely evades low-$K$ zones and follows primarily preferential pathways through relatively high-$K$ zones. The constant $K$ value is then set to 1.3 $m\,d^{-1}$, which was the uniform mean value suggested by Johansson et al. (2005) for the upper soil layer and for the soil – bedrock interface of Forsmark, based on field permeability testing and generic data. The soil – bedrock interface in this catchment is typically located at a depth of less than 5 m (Johansson, 2008).

Scenario 2 differs from and extends the scenario 1-based situation that has been considered in previous Forsmark studies (Persson and Destouni, 2009; Darracq et al., 2010a, b; Destouni et al., 2010). In scenario 2, the transport-encountered $K$ is statistically non-stationary, with local mean values of $K$ varying both among and along the transport pathways through the catchment, in accordance with available data on the geographical distribution of different soil types over the catchment (Jarsjö et al., 2008) and site-specific and generic data of typical $K$ values for the different soil types (Johansson 2008). In this scenario, the geometric mean value of $K$ is 0.71 m d$^{-1}$, and the standard deviation of ln$K$ is 1.8.

The two scenarios 1 and 2 have thus very different $K$ distributions (Fig. 1) that may bound many alternative representations of $K$ variability in a catchment. Stochastic $K$ fluctuations around the mean local $K$ values (constant in scenario 1 and variable in the non-stationary scenario 2) are not included in the present scenario analysis, for illustrative simplicity and because such fluctuations were found to have a relatively minor impact on the catchment-scale travel time distribution. Persson and Destouni (2009) have also previously investigated the effects of such stochastic fluctuations for transport from point sources in a scenario 1-situation, for which the relative importance of these fluctuations is the greatest.

For the present two scenarios we used the same methodology as described by Darracq et al. (2010a, b) and Destouni et al. (2010) to quantify the distributions of advective solute travel times from a uniform source input over the whole land surface of the Forsmark catchment to the nearest inland or coastal surface water. Specifically, we used high-resolution (10 × 10 m) elevation data to generate raster maps of ground slope and flow direction (local drain direction network). From these maps, we calculated advective solute travel times from each model cell through the groundwater to the nearest surface water. The advective solute travel time $\tau$ from each model cell location $\underset{\sim}{a}$, along the topographically derived flow and transport pathway, to the nearest downstream



surface water at distance $x_{\mathrm{CP}}$, was then calculated from the horizontal cell-to-cell flow path lengths, $\sum_{i=1 \text{ at } \underset{\sim}{a}}^{i=N \text{ at } X_{\mathrm{CP}}} \Delta x_i$, where $\Delta x_i$ is the flow length through each cell, and the estimated local mean flow and advective transport velocities along each transport pathway from $\underset{\sim}{a}$ to $x_{\mathrm{CP}}$. The local velocity was quantified as $v_i = \left[(K_i \cdot I_i)/n_i\right]$, and the associated $\tau$ increment through each model grid cell as $\Delta\tau_i = \Delta x_i \big/ v_i$, where $I_i$ is the local hydraulic gradient and $n_i$ is the local effective porosity.

For both scenarios, the effective porosity was set to be $n = 0.05$, as reported by Johansson (2008). The hydraulic gradient $I$ was set equal to the arithmetic average of the ground slope in all model cells within each one of the sub-catchments of a total of 8783 outlets to the surface water network or the sea. Darracq et al. (2010a) have previously investigated the effect of alternative hydraulic gradient scenarios for the Forsmark catchment, and the two resulting travel distributions from the present two $K$ scenarios (shown and discussed further in the Results section below) bound the different travel time distributions resulting from their different $I$ scenarios.

### 2.3 Quantification of mass delivery for physical-biogeochemical heterogeneity scenarios

Based on the estimated advective travel time distributions for the two different $K$ variability scenarios, we further quantified the total cumulative mass delivery to surface water from all possible pollutant input locations over the whole land surface area in the Forsmark catchment. For an attenuation scenario of constant first-order mass attenuation rate $\lambda$, we quantified the delivered mass fraction $\alpha$ from each model cell at location $\underset{\sim}{a}$ to the nearest surface water at $x_{\mathrm{CP}}$ as $\alpha = \exp(-\lambda\tau)$, where $\tau$ is the advective travel time along the pathway from $\underset{\sim}{a}$ to $x_{\mathrm{CP}}$, calculated as described above.

For the $K$ variability scenario 2, we also quantified the advective travel time-related mass delivery $\alpha$ for three different scenarios of variability in local attenuation rate $\lambda$ and its cross-correlation with local $K$: (i) $\lambda$ has perfect positive correlation with $K$ and is quantified as $\lambda = \lambda_g \cdot K / K_g$, where $\lambda_g$ and $K_g$ are the geometric mean values of $\lambda$ and $K$ over the catchment, respectively; (ii) $\lambda$ has perfect negative correlation with $K$ and is quantified as $\lambda = \lambda_g \cdot (-K / K_g)$; and (iii) $\lambda$ is an independent, lognormally distributed random variable with log variance $V[\ln\lambda] = V[\ln K]$. The local mass delivery $\alpha_i$ from each cell to the first downstream cell was then calculated as $\alpha = \exp(-\lambda_i \Delta\tau_i)$ and the total $\alpha$ along each cell-to-cell pathway from $\underline{a}$ to $x_{\mathrm{CP}}$ as $\alpha = \prod_{i=1 \text{ at } \underline{a}}^{i=N \text{ at } x_{\mathrm{CP}}} \alpha_i$.

## 3 Results

### 3.1 Travel time distributions

Figure 2 shows the maps and cumulative distributions of the advective solute travel times from every 10 × 10 m model cell in the Forsmark catchment area to the nearest inland or coastal surface water for the two $K$ variability scenarios (Fig. 1). Travel time statistics for the two scenarios are also summarised in Table 1. The distributions of advective solute travel times are very different for the two scenarios 1 and 2 (Fig. 2). These distributions bound all the different travel time distribution scenarios reported by Darracq et al. (2010a, b) for the Forsmark catchment, as well as for another investigated, nearby but much larger catchment in Sweden (the Norrström drainage basin). Those previously reported travel time distributions were calculated for different assumptions of hydraulic gradient variability and of the flow and transport interactions between shallow and deep groundwater along the subsurface pathways to the surface and coastal waters.

The travel time distribution for scenario 1 with constant $K$ shows the combined travel time spreading effect of the variability in transport pathway lengths and hydraulic gradients among the different transport pathways through the catchment. The travel time distribution for scenario 2 shows the added travel time spreading effect of the full $K$





variability across the catchment, where the flow and transport do not evade this variability by following relatively high-conductive preferential pathways as in scenario 1. However, note that even though the mean travel time is much greater in scenario 2 than in scenario 1, the fraction of very fast transport pathways, with a travel time to nearest surface water of $\tau \leq 0.01$ yr, is in fact larger in scenario 2 than in scenario 1. These fast pathways in scenario 2 originate from areas in the vicinity of surface water with shallow deposits of wave washed sand (Johansson, 2008) in which the estimated conductivity is larger than the constant $K$ value ($K = 1.3\,\mathrm{m\,d^{-1}}$) in scenario 1 (see Fig. 1).

### 3.2 Mass delivery for physical heterogeneity scenarios

Figure 3 shows, for the specific attenuation case of uniform first-order attenuation rate $\lambda$, the total, or catchment-average, mass delivery fraction, $\bar{\alpha}_{\mathrm{C}}$, to the nearest surface water from a uniform mass input over the entire land area in the Forsmark catchment, for a range of different catchment-characteristic products $\lambda\tau_g$, where $\tau_g$ is the geometric mean advective travel time to surface water in the catchment. Results are shown for the different travel time distributions of the $K$ variability scenarios 1 and 2, and for comparison also for the common approach in lumped hydrological modelling to just use a single representative (mean) travel time for a whole (sub)catchment (see for instance also discussions about this approach and its effects in Lindgren and Destouni (2004), Darracq and Destouni (2005, 2008), Destouni and Darracq (2006), Destouni et al. (2010)). To represent this lumped approach, where the travel time distribution around $\tau_g$ is neglected, the total mass delivery fraction to nearest surface water from the diffuse source input over whole catchment is calculated as $\bar{\alpha}_{\mathrm{C}} = \exp(-\lambda\tau_g)$.

In general, the mass delivery $\bar{\alpha}_{\mathrm{C}}$ estimated with a lumped, single travel time approach falls more rapidly toward zero as $\lambda\tau_g$ increases than in the variability-accounting scenarios 1 and 2. For $\lambda\tau_g$ in the order of 1 or greater, larger travel time variability increases the total mass delivery $\bar{\alpha}_{\mathrm{C}}$. Scenario 2 then yields the largest $\bar{\alpha}_{\mathrm{C}}$ because it has the largest fraction of transport pathways with advective travel times much longer than $\tau_g$, along which a significant mass fraction can reach the recipient, even for large characteristic attenuation product $\lambda\tau_g$. For $\lambda\tau_g$ smaller than 1, by contrast, larger travel time variability decreases the mass delivery $\bar{\alpha}_C$. Scenario 2 then results in the smallest $\bar{\alpha}_C$, (even though still quite close to that of scenario 1 and the single travel time approach) because it has the largest fraction of much longer travel times than $\tau_g$, where some mass is attenuated even for small $\lambda\tau_g$.

For comparison with the investigated $\lambda\tau_g$ range in Fig. 3, Table 2 shows examples of some typical orders of magnitude of attenuation rate $\lambda$ reported in the literature for different organic pollutants, metals and nutrients. Furthermore, Table 2 lists the associated order of magnitude of the catchment-characteristic product $\lambda\tau_g$ in the two $K$ variability scenarios 1 ($\tau_g = 0.73$ yr) and 2 ($\tau_g = 6.1$ yr). The reported attenuation rates for most substances range over large intervals, because the attenuation processes depend on environmental conditions (such as water flow velocity, microbial activity, and the availability of oxygen and other electron acceptors or donors) that vary within and between sites. In addition, estimates of attenuation rates in the field are based on approximations and simplified assumptions that may introduce considerable errors (Bekins et al., 1998; Suarez and Rifai, 1999; Washington and Cameron, 2001; Mulligan and Yong, 2004). Nevertheless, Table 2 demonstrates that the investigated $\lambda\tau_g$ range in this paper is relevant for a wide range of different environmental pollutants and characteristic catchment conditions; the latter because the investigated travel time pdfs bound a wide range of different possible catchment situations with regard to advective transport and its associated uncertainties (see comparisons between different scenarios and catchment examples in Darracq et al., 2010a, b). For the quantification of the waterborne transport of some compounds of interest in a specific (sub)catchment, the range of relevant reported attenuation rates can be narrowed through a more detailed assessment of the prevailing environmental conditions in relation to the ones reported at the sites where attenuation rates of these compounds have been estimated in previous studies. Table 2 further shows that for scenario 2 the catchment-relevant $\lambda\tau_g$ range for some substances under aerobic attenuation conditions may extend to even greater





values than the maximum $\lambda\tau_g = 1000$ shown in Fig. 3. If the prevailing catchment-scale $\tau$ variability is neglected or underestimated (Fig. 3), high-$\lambda\tau_g$ conditions and resulting underestimation of pollutant delivery $\bar{\alpha}_C$ may be more likely to occur in the field for these and other substances than low-$\lambda\tau_g$ conditions with $\bar{\alpha}_C$ overestimation.

### 3.3 Mass delivery for physical-biogeochemical heterogeneity scenarios

For the possibility that also $\lambda$ varies, along with $K$ and $\tau$, Fig. 4 shows for different $\lambda$ variability and $K$-correlation cases the resulting $\bar{\alpha}_C$ in scenario 2, relative to that in scenario 1, which has constant $K$ and $\lambda$, and smaller resulting $\tau$ variability (Fig. 2). For $\lambda\tau_g < 10$, the scenario 2 cases of negative or no $\lambda$–$K$ correlation yield pollutant mass delivery $\bar{\alpha}_C$ that is smaller than that of positive correlation or no $\lambda$ variability. The negative $\lambda$–$K$ correlation implies that the zones with smaller than average $K$ have larger than average attenuation rate $\lambda$, with both factors increasing pollutant attenuation relative to average conditions. In the case of no $\lambda$–$K$ correlation, where $\lambda$ in each model cell is an independent random variable, $\lambda$ is much greater than average along considerable parts of most transport pathways; this variability manifestation then results in more attenuated mass in total, and thereby smaller mass delivery $\bar{\alpha}_C$, compared to the constant $\lambda$ variability case for a wide range of average $\lambda\tau_g$ conditions. For positive $\lambda$–$K$ correlation, the zones with larger than average $\lambda$ associated with larger than average $K$, so that the $\lambda$ effect is to increase and the $K$ effect is to decrease pollutant attenuation; together these opposite effects may balance the resulting attenuation close to average $\lambda$ and $K$ conditions.

Comparison between the lower-panel maps in Fig. 4 specifically enables the identification of the main land areas within the catchment that are responsible for the mass-delivery divergence between the different $\lambda$ variability and $K$ correlation cases for low $\lambda\tau_g$ values. These are the green-coloured areas with mass delivery <0.01 % in the lower-right, negative-correlation map, which are instead red-coloured with mass delivery >50 % in the lower-left, positive-correlation map. These are also more generally the potential lowest-impact areas in the catchment, because the transport pathways from these areas to nearest surface/coastal water may be more or less forced to go through low-conductivity (smaller than average $K$) zones in different possible alternative transport scenarios, which are bounded by the extreme scenarios 1 and 2; with the possible exception of the positive $\lambda$–$K$ correlation case, these transport pathways will then have larger mass attenuation than the other transport pathways in the catchment.

Relative to scenario 1, in which $K$ is constant and the pollutant transport evades low-conductivity zones, all the $\lambda$ variability and correlation cases for scenario 2 yield smaller, or up to about the same, pollutant delivery $\bar{\alpha}_C$ for $\lambda\tau_g < 1$ (see middle curve plot in Fig. 4. As $\lambda\tau_g$ increases, the effects of $\lambda$ and $K$ variability on $\bar{\alpha}_C$ become opposite to those for low $\lambda\tau_g$. For larger $\lambda\tau_g$, more pollutant mass is of course attenuated on the average. The mass delivery to surface and coastal waters becomes insignificant from an increasing part of the catchment, and an increasing fraction of the total mass delivery comes from areas with relatively short pathway lengths to nearest surface or coastal water and greater than average hydraulic gradient $I$ and conductivity $K$. The negative $\lambda$–$K$ correlation case yields the largest mass delivery from such high-$K$ areas with particularly short travel times to the recipient. These areas then emerge as potential hotspots for pollutant loading from the catchment; these are the red-coloured areas, with mass delivery >50 % for $\lambda\tau_g = 1000$ in the negative-correlation case, which are almost entirely green-coloured, with mass delivery <1 % in the positive correlation case (Fig. 4). These potential hotspots are responsible for the much higher (up to factor 1000 for $\lambda\tau_g = 1000$; Fig. 4) total mass load into surface/coastal waters for large $\lambda\tau_g$ in scenario 2 than in scenario 1, with its lower $\tau$ variability and constant $\lambda$ (and the even greater relative difference between mass load in scenario 2 and that for constant $\tau$ and $\lambda$, shown in Fig. 3). Even though not particularly high in relation to the total input mass (maximum $\bar{\alpha}_C = 0.023$ for $\lambda\tau_g = 1000$; Fig. 4), a factor 1000 greater pollutant load can shift environmental and health risk assessments, from no risk to large risk, for highly toxic pollutants with environmental limit values at or near detection level.

In general, across the whole $\lambda\tau_g$ range in Fig. 4, the high $\tau$ variability scenario 2 with constant $\lambda$ yields $\bar{\alpha}_C$ close to the maximum-$\bar{\alpha}_C$ results associated with either the



positive (for $\lambda\tau_g < 10$) or the negative (for $\lambda\tau_g < 10$) $\lambda$–$K$ correlation cases. A scenario of high physical $K$–$\tau$ variability combined with a constant $\lambda$ value, representative of relevant average biogeochemical attenuation conditions, can thus be considered as a reasonable conservative scenario assumption when field data and information is lacking for more precisely determining actual $K$–$\tau$ variability and $\lambda$–$K$ correlation. Furthermore, the advective travel time $\tau$ map of a high $K$–$\tau$ variability scenario may also be directly (i.e., without further attenuation calculations and mass delivery mapping for different $\lambda$–$K$ correlation cases) useful for at least an approximate identification of potential hotspot zones for large average $\lambda\tau_g$ (red in upper-left map, Fig. 4) and low-impact zones for small average $\lambda\tau_g$ (green in lower-right map, Fig. 4). In the present catchment example, these zones are indeed directly identifiable from the $\tau$ map for scenario 2: compare the areas with the shortest and the longest travel times in the lower map of Fig. 2 with the red hotspot areas in the upper-left map and the green low-impact areas in the lower-right map of Fig. 4, respectively.

## 4 Conclusions

We have developed and shown the applicability of a scenario analysis approach to quantify and map the effects of physical and biogeochemical variability, cross-correlation and uncertainty on expected mass loading from diffuse sources. The approach is useful when field data and information is lacking for reliable determination of actual physical and biogeochemical variability and cross-correlation conditions in a catchment. It enables identification of conservative assumptions, uncertainty ranges, as well as pollutant/nutrient input locations and situations for which further investigations are most needed in order to reduce the uncertainty range.

The investigated variability scenarios have provided some relevant statistical distributions, bounding a range of different possible advective travel time statistics for diffuse hydrological mass transport from spatially widespread sources at and below the land surface, through soil and groundwater, to surface and coastal waters. Furthermore, the combined physical (advective) transport scenarios and mass attenuation cases in this study bound a wide range of different catchment conditions and types of pollutants and nutrients that may be accidentally, occasionally or continuously released from diffuse sources, as a result of current and/or historic human activities and remaining pollution legacies.

The results show that neglect or underestimation of the physical variability in subsurface hydraulic properties and resulting advective travel times implies substantial risk to underestimate pollutant and nutrient loading to downstream surface and coastal waters. This is particularly true for relatively high catchment-characteristic product ($\lambda\tau_g > 10$) between average attenuation rate and average advective travel time, for which mass delivery would be near zero under assumed transport homogeneity but can be orders of magnitude higher for variable transport conditions.

The results for the present scenario 2 of high physical advection variability (expressed here in terms of $K$ and $\tau$ variability) demonstrates that, for many environmental pollution/eutrophication problems, smaller natural attenuation and thereby larger loading of remaining pollutant/nutrient mass may occur in pathways that are faster or much faster than indicated by average flow and transport conditions, even if the average conditions are chosen to represent relatively fast, preferential pathways (as in the present scenario 1, with about an order of magnitude smaller geometric mean travel time than scenario 2). The study results also show that such a scenario of high physical advection variability (here scenario 2), combined with a relevant average biogeochemical attenuation rate, may be a generally reasonable, conservative assumption for estimating maximum diffuse loading mass loading when the prevailing physical and biogeochemical variability and cross-correlation are uncertain. As done here for scenario 2, a scenario of high advection variability can be constructed by use of the finest resolved available data on soil variability, which are further translated into a hydraulic conductivity and associated travel time distribution scenario. Alternatively, fine-resolved variability in local topographic slopes can be translated into a hydraulic gradient and associated



travel time distribution scenario, as done by Darracq et al. (2010a), yielding a similar high-variability travel time distribution to that for the present scenario 2.

Our results further show that the advective travel time map for the high advection variability scenario 2 directly identifies hotspot areas with large potential mass loading to downstream surface and coastal waters, and their opposite, potential lowest-impact areas within a catchment. Such substance-independent, high-variability calculations and mapping of advective travel times can thus be useful for at least approximate predictive identification of the parts of a catchment area where pollutant and nutrient releases are most and least likely to contribute much to pollution or eutrophication of downstream surface and coastal water systems, and where environmental protection/remediation measures may be most and least needed and effective.

*Acknowledgements.* We thank the Swedish Research Council (VR; contract number 60436601) for financial support of this work, which has also been carried out within the linked frameworks of Stockholm University's Strategic Environmental Research Projects EkoKlim and BEAM.

## References

Andricevic, R. and Cvetkovic, V.: Evaluation of risk from contaminants migrating by ground water, Water Resour. Res., 32, 611–621, 1996.

Arheimer, B., Löwgren, M., Pers, B. C., and Rosberg, J.: Integrated catchment modeling for nutrient reduction: scenarios showing impacts, potential and cost of various measures, Ambio, 34, 513–520, 2005.

Aronson, D. and Howard, P. H.: Anaerobic biodegradation of organic chemicals in groundwater: A summary of field and laboratory studies, Syracuse Research Corporation, North Syracuse, NY, USA, 1997.

Aronson, D., Citra, M., Shuler, K., Printup, H., and Howard, P. H.: Aerobic biodegradation of organic chemicals in environmental media: A summary of field and laboratory studies, Syracuse Research Corporation, North Syracuse, NY, USA, 1999.

Baresel, C. and Destouni, G.: Uncertainty-accounting environmental policy and management of water systems, Environ. Sci. Technol., 41(10), 3653–3659, doi:10.1021/es061515e, 2007.
Baresel, C. and Destouni, G.: Diffuse subsurface zinc loads from mining areas in the Dalälven River Basin, Sweden, Hydrol. Res., 40(5), 445–453, doi:10.2166/nh.2009.013, 2009.
Baresel, C., Destouni, G., and Gren, I.-M.: The influence of metal source uncertainty on cost-effective allocation of mine water pollution abatement in catchments, J. Environ. Manage., 78(2), 138–148, doi:10.1016/j.jenvman.2005.03.013, 2006.
Basu, N. B., Destouni, G., Jawitz, J. W., Thompson, S. E., Loukinova, N. V., Darracq, A., Zanardo, S., Yaeger, M. A., Sivapalan, M., Rinaldo, A., and Rao, P. S. C.: Nutrient loads exported from managed catchments reveal emergent biogeochemical stationarity, Geophys. Res. Lett., 37, L23404, doi:10.1029/2010GL045168, 2010.
Batchelor, B., Valdés, J., and Araganth, V.: Stochastic risk assessment of sites contaminated by hazardous waste, J. Environ. Eng., 124, 380–388, 1998.
Bayer-Raich, M., Jarsjö, J., Liedl, R., Ptak, T., and Teutsch, G.: Integral pumping test analyses of linearly sorbed groundwater contaminants using multiple wells: Inferring mass flows and natural attenuation rates, Water Resour. Res., 42, W08411, doi:10.1029/2005WR004244, 2006.
Bekins, B. A., Warren, E., and Godsy, E. M.: A comparison of zero-order, first-order, and Monod biotransformation models, Ground Water, 36(2), 261–268, 1998.
Bergknut, M., Meijer, S., Halsall, C., Ågren, A., Laudon, H., Köhler, S., Jones, K. C., Tysklind, M., and Wiberg, K.: Modelling the fate of hydrophobic organic contaminants in a boreal forest catchment: A cross disciplinary approach to assessing diffuse pollution to surface waters, Environ. Pollut., 158, 2964–2969, 2010.
Beven, K.: How far can we go in distributed hydrological modelling?, Hydrol. Earth Syst. Sci., 5, 1–12, doi:10.5194/hess-5-1-2001, 2001.
Beven, K. J.: A manifesto for the equifinality thesis, J. Hydrol., 320, 18–36, 2006.
Beven, K. J.: Preferential flow and travel time distributions: defining adequate hypothesis tests for hydrological models, Hydrol. Process., 24, 1537–1547, 2010.
Botter, G., Bertuzzo, E., Bellin, A., and Rinaldo, A.: On the Lagrangian formulations of reactive solute transport in the hydrologic response, Water Resour. Res., 41, W04008, doi:10.1029/2004WR003544, 2005.
Botter, G., Settin, T., Marani, M., and Rinaldo, A.: A stochastic model of Nitrate transport and cycling at basin scale, Water Resour. Res., 42, W04415, doi:10.1029/2005WR004599,





2006.
Botter, G., Bertuzzo, E., and Rinaldo, A.: Transport in the hydrologic response: travel time distributions, soil moisture dynamics and the old water paradox, Water Resour. Res., 46(3), W03514, doi:10.1029/2009WR008371, 2010.
Bring, A. and Destouni, G.: Hydrological and hydrochemical observation status in the pan-Arctic drainage basin, Polar Res., 28, 327–338, 2009.
Bring, A. and Destouni, G.: Relevance of hydro-climatic change projection and monitoring for assessment of water cycle changes in the Arctic, Ambio, doi:10.1007/s13280-010-0109-1, in press, 2011.
Chang, C. M., Kemblowski, M. W., and Urroz, G. E.: Transient stochastic analysis of biodegradable contaminant transport: first-order decay, Transport Porous Med., 35(1), 1–14, 1999.
Chapell, F. H.: The significance of microbial processes in hydrology and geochemistry, Hydrogeol. J., 8, 41–46, 2000.
Costanza, R.: Visions of alternative (unpredictable) futures and their use in policy analysis, Conserv. Ecol. online, 4(1), http://www.ecologyandsociety.org/vol4/iss1/art5/index.html, 2000.
Cozzarelli, I. M., Herman, J. S., Baedecker, M. J., and Fischer, J. M.: Geochemical heterogeneity of a gasoline-contaminated aquifer, J. Contam. Hydrol., 40, 261–284, 1999.
Cunningham, J. A. and Fadel, Z. J.: Contaminant degradation in physically and chemically heterogeneous aquifers, J. Contam. Hydrol., 94, 293–304, 2007.
Cvetkovic, V. and Dagan, G.: Transport of kinetically sorbing solute by steady random velocity in heterogeneous porous formations, J. Fluid Mech., 265, 189–215, 1994.
Cvetkovic, V. and Shapiro, A.: Mass arrival of sorptive solute in heterogeneous porous media, Water Resour. Res., 26, 2057–2067, 1990.
Cvetkovic, V., Dagan, G., and Shapiro, A. M.: A solute flux approach to transport in heterogeneous formations 2, Uncertainty analysis, Water Resour. Res., 28, 1377–1388, 1992.
Cvetkovic, V., Ceng, H., and Wen, X.-H.: Analysis of non-linear effects on tracer migration in heterogeneous aquifers using Lagrangian travel time statistics, Water Resour. Res., 32(6), 1671–1680, 1996.
Dagan, G.: Flow and Transport in Porous Formations, Springer Verlag, Berlin, 1989.
Darracq, A. and Destouni, G.: In-stream nitrogen attenuation: model-aggregation effects and implications for coastal nitrogen impacts, Environ. Sci. Technol., 39, 3716–3722, 2005.
Darracq, A. and Destouni, G.: Physical versus biogeochemical interpretations of Nitrogen and

Phosphorus attenuation in streams and its dependence on stream characteristics, Global Biogeochem. Cy., 21, GB3003, doi:10.1029/2006GB002901, 2007.
Darracq, A., Greffe, F., Hannerz, F., Destouni, G., and Cvetkovic, V.: Nutrient transport scenarios in a changing Stockholm and Mälaren valley region, Water Sci. Technol., 51(3–4), 31–38, 2005.
Darracq, A., Lindgren, G. A., and Destouni, G.: Long-term development of phosphorus and nitrogen loads through the subsurface and surface water systems of drainage basins, Global Biogeochem. Cy., doi:10.1029/2007GB003022, 2008.
Darracq, A., Destouni, G., Persson, K., Prieto, C., and Jarsjö, J.: Quantification of advective solute travel times and mass transport through hydrological catchments, Environ. Fluid Mech., 10, 103–120, doi:10.1007/s10652-009-9147-2, 2010a.
Darracq, A., Destouni, G., Persson, K., Prieto, C., and Jarsjö, J.: Scale and model resolution effects on the distributions of advective solute travel times in catchments, Hydrol. Process., 24, 1697–1710, doi:10.1002/hyp.7588, 2010b.
Destouni, G.: Prediction uncertainty in solute flux through heterogeneous soil, Water Resour. Res. 28(3), 793–801, 1992.
Destouni, G.: Stochastic modelling of solute flux in the unsaturated zone at the field scale, J. Hydrol., 143, 45–61, 1993.
Destouni, G. and Cvetkovic, V.: Field scale mass arrival of sorptive solute into the groundwater, Water Resour. Res., 27(6), 1315–1325, 1991.
Destouni, G. and Graham, W.: Solute transport through an integrated heterogeneous soil-groundwater system, Water Resour. Res., 31, 1935–1944, 1995.
Destouni, G. and Graham, W.: The influence of observation method on local concentration statistics in the subsurface, Water Resour. Res., 33(4), 663–676, 1997.
Destouni, G., Simic, E., and Graham, W.: On the applicability of analytical methods for estimating solute travel time statistics in nonuniform groundwater flow, Water Resour. Res., 37, 2303–2308, 2001.
Destouni, G., Lindgren, G., and Gren, I. M.: Effects of inland nitrogen transport and attenuation modeling on coastal nitrogen load abatement, Environ. Sci. Technol., 40, 6208–6214, doi:10.1021/es060025j, 2006.
Destouni, G., Shibuo, Y., and Jarsjö, J.: Freshwater flows to the sea: Spatial variability, statistics and scale dependence along coastlines, Geophys. Res. Lett., 35, L18401, doi:10.1029/2008GL035064, 2008a.





Destouni, G., Hannerz, F., Prieto, C., Jarsjö, J., and Shibuo, Y.: Small unmonitored near-coastal catchment areas yielding large mass loading to the sea, Global Biogeochem. Cy., 22, GB4003, doi:10.1029/2008GB003287, 2008b.
Destouni, G., Persson, K., Prieto, C., and Jarsjö, J.: General quantification of catchment-scale nutrient and pollutant transport through the subsurface to surface and coastal waters, Environ. Sci. Technol., 44(6), 2048–2055, 2010.
Edwards, A. C. and Withers, P. J. A.: Transport and delivery of suspended solids, nitrogen and phosphorus from various sources to freshwaters in the UK, J. Hydrol., 350, 144–153, 2008.
Eggleston, J. R. and Rojstaczer, S. A.: Can we predict subsurface mass transport?, Environ. Sci. Technol., 34, 4010–4017, 2000.
Eriksson, N. and Destouni, G.: Combined effects of dissolution kinetics, secondary mineral precipitation, and preferential flow on copper leaching from mineral waste rock, Water Resour. Res., 33(3), 471–483, 1997.
Essaid, H. I., Cozzarell, I. M., Eganhouse, R. P., Herkelrath, W. N., Bekins, B. A., and Delin, G. N.: Inverse modeling of BTEX dissolution and biodegradation at the Bemidji, MN crude-oil spill site, J. Contam. Hydrol., 67, 269–299, 2003.
Ganoulis, J.: Risk Analysis of Water Pollution: Second, revised and expanded edition, WILEY-VCH Verlag, Weinheim, 2009.
Graham, W., Destouni, G. Demmy, G., and Foussereau, X.: Prediction of local concentration statistics in variably saturated soils: Influence of observation scale and comparison with field data, J. Contam. Hydrol., 32(1–2), 177–199, 1998.
Grabs, T., Seibert, J., Bishop, K., and Laudon, H.: Modeling spatial patterns of saturated areas: A comparison of the topographic wetness index and a dynamic distributed model, J. Hydrol., 373(1–2), 15–23, 2009.
Gren, I. M., Destouni, G., and Sharin, H.: Cost effective management of stochastic coastal water pollution, Environ. Model. Assess., 5(4), 193–203, 2000.
Gren, I-M., Destouni, G., and Tempone, R.: Cost effective policies for alternative distributions of stochastic water pollution, J. Environ. Manage., 66, 145–157, 2002.
Gupta, A. and Cvetkovic, V.: Temporal moment analysis of tracer discharge in streams: Combined effect of mass transfer and morphology, Water Resour. Res., 36, 2985–2997, 2000.
Gupta, A. and Cvetkovic, V.: Material transport from different sources in a network of streams through a catchment, Water Resour. Res., 38, 1098, doi:10.1029/2000WR000064, 2002.
Hagemann, S. and Jacob, D.: Gradient in the climate change signal of European discharge

predicted by a multi-model ensemble, Climatic Change, 81, 309–327, 2007.
Hannerz, F. and Destouni, G.: Spatial characterization of the Baltic Sea Drainage Basin and its unmonitored catchments, Ambio, 214–219, 2006.
Jacob, D., Bärring, L., Christensen, O. B., Christensen, J. H., Hagemann, S., Hirschi, M., Kjellström, E., Lenderink, G., Rockel, B., Schär, C., Seneviratne, S. I., Somot, S., van Ulden, A., and van den Hurk, B.: An inter-comparison of regional climate models for Europe: design of the experiments and model performance, Climatic Change, 81(Supplement 1), 31–52, 2007.
Jarsjö, J. and Bayer-Raich, M.: Estimating plume degradation rates in aquifers: effect of propagating measurement and methodological errors, Water Resour. Res., 44, W02501, doi:10.1029/2006WR005568, 2008.
Jarsjö, J., Destouni, G., and Yaron, B.: On the relation between viscosity and hydraulic conductivity for volatile organic liquid mixtures in soils, J. Contam. Hydrol., 25(1–2), 113–127, 1997.
Jarsjö, J., Bayer-Raich, M., and Ptak, T.: Monitoring groundwater contamination and delineating source zones at industrial sites: Uncertainty analyses using integral pumping tests, J. Contam. Hydrol., 79, 107–134, 2005.
Jarsjö, J., Shibuo, Y., Prieto, C., and Destouni, G.: GIS-based modelling of coupled groundwater – surface water hydrology in the Forsmark and Simpevarp areas, Swedish Nuclear Fuel and Waste Management Co Report R-05-67, Stockholm, 2006.
Jarsjö, J., Destouni, G., Persson, K., and Prieto, C.: Solute transport in coupled inland-coastal water systems: General conceptualization and application to Forsmark, Swedish Nuclear Fuel and Waste Management Co Report R-07-65, Stockholm, 2007.
Jarsjö, J., Shibuo, Y., and Destouni, G.: Spatial distribution of unmonitored inland water flows to the sea. J. Hydrol., 348, 59–72, 2008.
Jöborn, A., Danielsson, I., Arhemier, B., Jonsson, A., Larsson, M., Lundqvist, J. L., Löwgren, M., and Tonderski, K.: Integrated water management for eutrophication control: public participation, pricing policy, and catchment modelling, Ambio 34, 482–488, 2005.
Johansson, P.-O.: Description of surface hydrology and near-surface hydrogeology at Forsmark. Site descriptive modelling, SDM-Site Forsmark. Swedish Nuclear Fuel and Waste Management Co Report R-08-08, 2008.
Johansson, P.-O. and Öhman, J.: Presentation of meteorological, hydrological and hydrogeological monitoring data from Forsmark: Site descriptive modelling – SDM-Site Forsmark,



Swedish Nuclear Fuel and Waste Management Co Report R-08-10, 2008.
Johansson, P.-O., Werner, K., Bosson, E., and Juston, J.: Description of climate, surface hydrology, and near-surface hydrology. Preliminary site description. Forsmark area – version 1.2. Swedish Nuclear Fuel and Waste Management Co Report R-05-06, 2005.
Lindgren, G. A., Destouni, G., and Miller, A. V.: Solute transport through the integrated groundwater-stream system of a catchment, Water Resour. Res., 40, W03511, doi:10.1029/2003WR002765, 2004.
Lindgren, G. A., Destouni, G., and Darracq, A.: Inland subsurface water system role for coastal nitrogen load dynamics and abatement responses, Environ. Sci. Technol., 41(7), 2159–2164, 2007.
Kaluarachchi, J. J., Cvetkovic, V., and Berglund, S.: Stochastic analysis of oxygen- and nitrate-based biodegradation of hydrocarbons in aquifers, J. Contam. Hydrol., 41, 335–365, 2000.
Kyselý, J. and Beranová, R.: Climate change effects on extreme precipitation in central Europe: uncertainties of scenarios based on regional climate models, Theor. Appl. Climatol., 95, 361–374, 2009.
Macleod, C. J. A., Scholefield, D., and Haygarth, P. M.: Integration for sustainable catchment management, Sci. Total Environ., 373, 591–602, 2007.
Malmström, M., Destouni, G., Banwart, S., and Strömberg, B.: Resolving the scale-dependence of mineral weathering rates, Environ. Sci. Technol., 34, 1375–1378, 2000.
Malmström, M. E., Destouni, G., and Martinet, P.: Modeling expected solute concentration in randomly heterogeneous flow systems with multicomponent reactions, Environ. Sci. Technol., 38, 2673–2679, 2004.
Malmström, M. E., Berglund, S., and Jarsjö, J.: Combined effects of spatially variable flow and mineralogy on the attenuation of acid mine drainage in groundwater, Appl. Geochem., 23, 1419–1436, doi:10.1016/j.apgeochem.2007.12.029, 2008.
McDonnell, J. J., McGuire, K., Aggarwal, P., Beven, K., Biondi, D., Destouni, G., Dunn, S., James, A., Kirchner, J., Kraft, S., Lyon, S., Malowszewski, P., Newman, L., Pfister, L., Rinaldo, A., Rodhe, A., Sayama, T., Seibert, J., Soloman, K., Soulsby, C., Stewart, M., Tetzlaff, D., Tobin, C., Troch, P., Weiler, M., Western, A., Wörmann, A., and Wrede, S.: How old is stream water? Open questions in catchment transit time conceptualisation, modelling and analysis, Hydrol. Process., 24, 1745–1754, 2010.
McGuire, K. J., McDonnell, J. J., Weiler, M., Kendall, C., McGlynn, B. L., Welker, J. M., and Seibert, J.: The role of topography on catchment-scale water residence time, Water Resour.

Res., 41(5), W05002.1–W05002.14, 2005.
Miralles-Wilhelm, F. and Gelhar, L. W.: Stochastic analysis of transport and decay of a solute in heterogeneous aquifers, Water Resour. Res., 32(12), 3451–3459, 1996.
Molénat, J. and Gascuel-Odoux, C.: Modelling flow and nitrate transport in groundwater for the prediction of water travel times and of consequences of land use evolution on water quality. Hydrol. Process., 16(2), 479–492, 2002.
Mulligan, C. N. and Yong, R. N.: Natural attenuation of contaminated soils, Environ. Int., 30, 587–601, 2004.
Olli, G. and Destouni, G.: Long-term heavy metal loading to near-shore sediments, Water Air Soil Poll., 192, 105–116, doi:10.1007/s11270-008-9638-7, 2008.
Oreskes, N., Shrader-Frechette, K., and Belitz, K.: Verification, validation, and confirmation of numerical models in the earth sciences, Science, 263, 641–646, 1994.
Persson, K. and Destouni, G.: Propagation of water pollution uncertainty and risk from the subsurface to the surface water system of a catchment, J. Hydrol., 377, 434–444, doi:10.1016/j.hydrol.2009.09.001, 2009.
Popper, S. W, Lempert, R. J., and Bankes, S. C.: Shaping the future, Sci. Am., 292(4), 66–71, 2005.
Prieto, C. and Destouni, G.: Is submarine groundwater discharge predictable?, Geophys. Res. Lett., 38, L01402, doi:10.1029/2010GL045621, 2011.
Prieto, C., Kotronarou, A., and Destouni, G.: The influence of temporal hydrological randomness on seawater intrusion in coastal aquifers, J. Hydrol., 330, 285–300, 2006.
Refsgaard, J. C., van der Sluijs, J. P., Brown, J., and van der Keur, P.: A framework for dealing with uncertainty due to model structure error, Adv. Water Resour., 29, 1586–1597, 2006.
Rinaldo, A., Botter, G., Bertuzzo, E., Uccelli, A., Settin, T., and Marani, M.: Transport at basin scales: 1. Theoretical framework, Hydrol. Earth Syst. Sci., 10, 19–29, doi:10.5194/hess-10-19-2006, 2006.
Rubin, Y.: Transport in heterogeneous porous media: Prediction and uncertainty, Water Resour. Res., 27, 1723–1738, 1991.
Rubin, Y.: Applied Stochastic Hydrogeology, Oxford University Press, New York, 2003.
Shapiro, A. M. and Cvetkovic, V.: Stochastic analysis of solute arrival time in heterogeneous porous media, Water Resour. Res., 24, 1711–1718, 1988.
Simmons, C. S., Ginn, T. R., and Wood, B. D.: Stochastic-convective transport with nonlinear reaction: Mathematical framework, Water Resour. Res., 31, 2675–2688, 1995.





Sinkkonen, S. and Paasivirta, J.: Degradation half-life times of PCDDs, PCDFs and PCBs for environmental fate modeling, Chemosphere, 40, 943–949, 2000.
SKB: Description of surface systems: Preliminary site description. Forsmark area – version 1.2. Swedish Nuclear Fuel and Waste Management Co Report R-05-03, 2005.
SKB: Site description of Forsmark at completion of the site investigation phase: SDM-Site Forsmark. Swedish Nuclear Fuel and Waste Management Co Report TR-08-05, 2008.
Suarez, M. P. and Rifai, H. S.: Biodegradation rates for fuel hydrocarbons and chlorinated solvents in groundwater, Bioremediation Journal, 3, 337–362, 1999.
Swart, R., Raskin, P., and Robinson, J.: The problem of the future: sustainability science and scenario analysis, Global Environ. Change, 14, 137–146, 2004.
Tompson, A. F. B., Bruton, C. J., Pawloski, G. A., Smith, D. K., Bourcier, W. L., Shumaker, D. E., Kersting, A. B., Carle, S. F., and Maxwell, R. M.: On the evaluation of groundwater contamination from underground nuclear tests, Environ. Geol., 42, 235–247, 2002.
de Vries, B. J. M.: Scenarios: guidance for an uncertain and complex world?, in: Sustainability or Collapse? An Integrated History and Future of People on Earth, edited by: Costanza, R., Graumlich, L. J., and Steffen, W., MIT Press, pp. 379–397, 2007.
Washington, J. W. and Cameron, B. A.: Evaluating degradation rates of chlorinated organics in groundwater using analytical models, Environ. Toxicol. Chem., 20(9), 1909–1915, 2001.
Werner, K., Johansson, P., Brydsten, L., Bosson, E., Berglund, S., Tröjbom, M., and Nyman, H.: Recharge and discharge of near-surface hydrology, Swedish Nuclear Fuel and Waste Management Co Report R-07-08, 2007.
de Wit, M., Meinardi, C., Wendland, F., and Kunkel, R.: Modelling water fluxes for the analysis of diffuse pollution at the river basin scale, Hydrol. Process., 14, 1707–1723, 2000.
Yabusaki, S. B., Steefel, C. I., and Wood, B. D.: Multidimensional, multicomponent, subsurface reactive transport in nonuniform velocity fields: code verification using an advective reactive streamtube approach, J. Contam. Hydrol., 30(3), 299–331, 1998.
Young, M. N., Leemans, R., Boumans, R. M. J., Costanza, R., de Vries, B. J. M., Finnigan, J., Svedin, U., and Young, M. D.: Group report: future scenarios of human-environment systems, in: Sustainability or Collapse? An Integrated History and Future of People on Earth, edited by: Costanza, R., Graumlich, L. J., Steffen, W., MIT Press, 446–470, 2007.

**Table 1.** Statistics of advective solute travel time $\tau$ to nearest surface water for the two $K$ variability scenarios in Fig. 1.

| | Geometric mean $\tau$ (yr) | Standard deviation of $\ln\tau$ | Arithmetic mean $\tau$ (yr) | Coefficient of variation of $\tau$ |
|---|---|---|---|---|
| Scenario 1 | 0.73 | 1.5 | 1.5 | 1.1 |
| Scenario 2 | 6.1 | 2.9 | 66 | 1.9 |





**Table 2.** Examples of pollutants and nutrients with corresponding estimates of first-order attenuation rate $\tau$ from reported field studies, and associated order of magnitude of the attenuation product $\lambda\tau_g$ for scenarios 1-2 in the Forsmark catchment area.

| Example pollutants (for which given $\lambda$ is consistent with field observations of $\lambda$) | Attenuation rate ($yr^{-1}$) | Attenuation product | |
|---|---|---|---|
| | | Scenario 1 $\tau_g = 0.73$ yr | Scenario 2 $\tau_g = 6.1$ yr |
| Polychlorinated biphenyls (PCBs)[1], benzene[anaer;2,3], ethylbenzene[anaer;2,3], toluene[anaer;2,3,4], m,p,o-xylene[anaer;2,3], vinyl chloride[anaer;2,3], trichloroethene[anaer;2,3], naphthalene[anaer;2,4] | $\leq 0.014$ | $\leq 0.01$ | $\leq 0.1$ |
| Polychlorinated biphenyls (PCBs)[1], zinc[5,6], phosphorus[7], benzene[anaer;2,3,8,9], ethylbenzene[anaer;2,3,9], toluene[anaer;2,3,4], m,p,o-xylene[anaer;2,3], vinyl chloride[anaer;2,3], trichloroethene[anaer;2,3], naphthalene[anaer;2,4], acenaphthylene[anaer;4] | 0.14 | 0.1 | 1 |
| Cadmium[5], copper[5], zinc[5,6], phosphorus[7,10], nitrogen[10], benzene[2,3,4,8,9,11], ethylbenzene[2,3,9,11], toluene[2,3,4,11,12], o-xylene[2,3,11], m,p-xylene[2,9,11], vinyl chloride[2,8], trichloroethene[2,8,11], naphthalene[2,4,11], acenaphthylene[4,12], fluoranthene[11] | 1.4 | 1 | 10 |
| Benzene[aer;3,9,11], toluene[2,3,11,12], ethylbenzene[2,3,12], m,p,o-xylene[2,3,4,9,11,12], vinyl chloride[2,3], trichloroethene[2,3,11], naphthalene[2,12], acenaphthylene[12], acenaphthene[12], anthracene[12], fluoranthene[4,12] | 14 | 10 | 100 |
| Benzene[aer;3,12], toluene[aer;3,11,12], ethylbenzene[aer;3], trichloroethene[aer;3,11], vinyl chloride[aer;3] | 140 | 100 | 1000 |
| Benzene [aer;3], toluene[aer;3,11], ethylbenzene[aer;3] | $\geq 1400$ | $\geq 1000$ | $\geq 10000$ |

[1] Sinkkonen and Paasivirta (2000);, [2] Aronson and Howard (1997); [3] Suarez and Rifai (1999); [4] Rogers et al. (2002); [5] Baresel et al. (2006); [6] Baresel and Destouni (2007); [7] Destouni et al. (2010); [8] Mulligan and Yong (2004); [9] Essaid et al. (2003),[10] Darracq et al. (2008)[11]; Aronson et al. (1999); [12] Bayer-Raich et al. (2006); [aer] Mainly relevant for aerobic conditions, [anaer] Mainly relevant for anaerobic conditions.

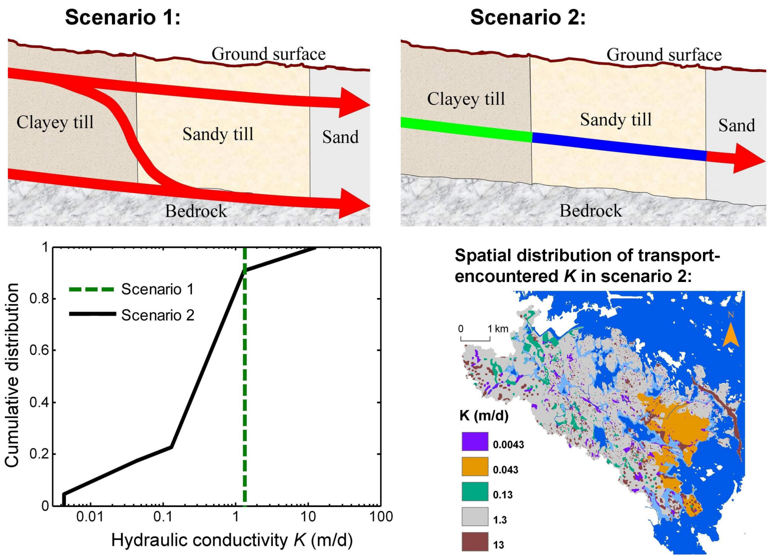


**Fig. 1.** Two scenarios of variability in saturated hydraulic conductivity, $K$, as encountered by the main flow and transport pathways (up) and their resulting cumulative $K$ distribution (down left) in the Forsmark catchment (map, down right). Different arrow colours in the schematic illustrations of main flow and transport pathways in the different scenarios represent different transport velocities. Scenario 1 (constant $K$) represents transport that occurs predominantly in high-conductivity aquifer zones, such as near the soil surface, at the soil-bedrock interface, and/or other inter-connected preferential flow paths. Scenario 2 (spatially variable, statistically non-stationary $K$) represents transport through soil and aquifer zones where $K$ varies spatially according to the available information of soil cover and average permeability of each soil type.





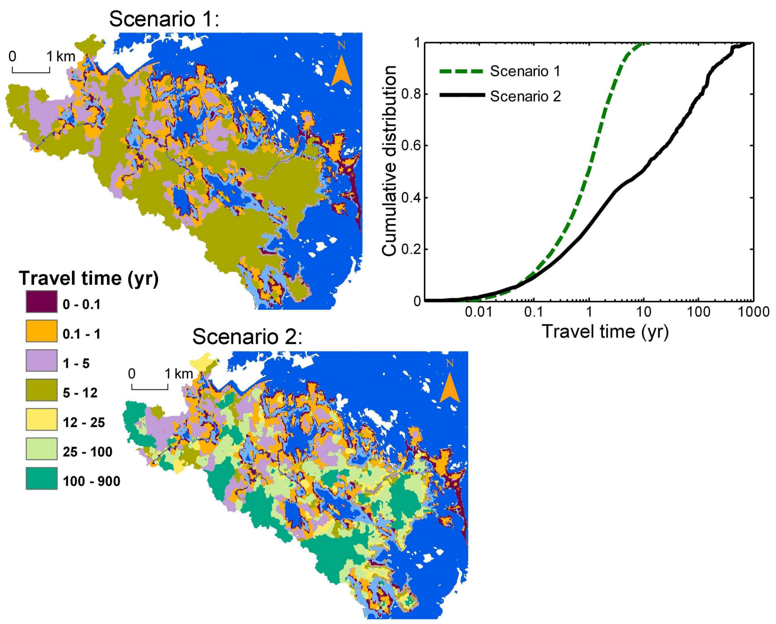


**Fig. 2.** The maps show advective travel times from different input locations in the Forsmark catchment to nearest surface water (inland or coastal) for the two considered $K$ variability scenarios. The graph shows the resulting cumulative distributions of travel time to surface water from all upstream input locations (model cells).

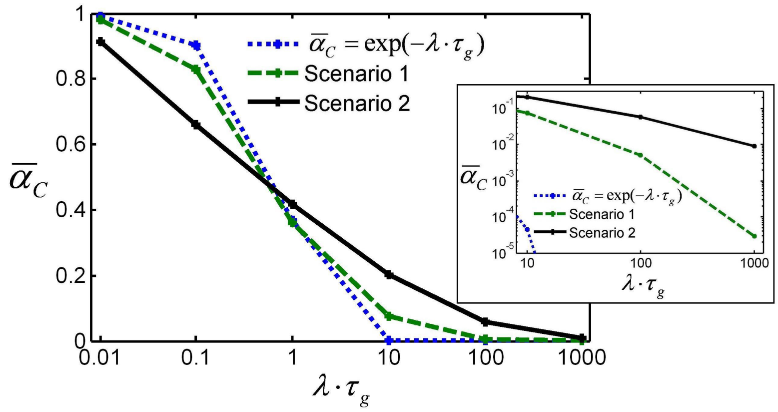


**Fig. 3.** Total (catchment-average) mass delivery fraction to nearest surface water from all upstream input locations in the Forsmark catchment, $\bar{\alpha}_C$, under the assumption of constant $\lambda$ for the two considered scenario with regards to $K$ variability, and for a calculation approach where the travel time variability around the geometric mean $\tau_g$ is neglected so that $\bar{\alpha}_C = \exp(-\lambda\tau_g)$.



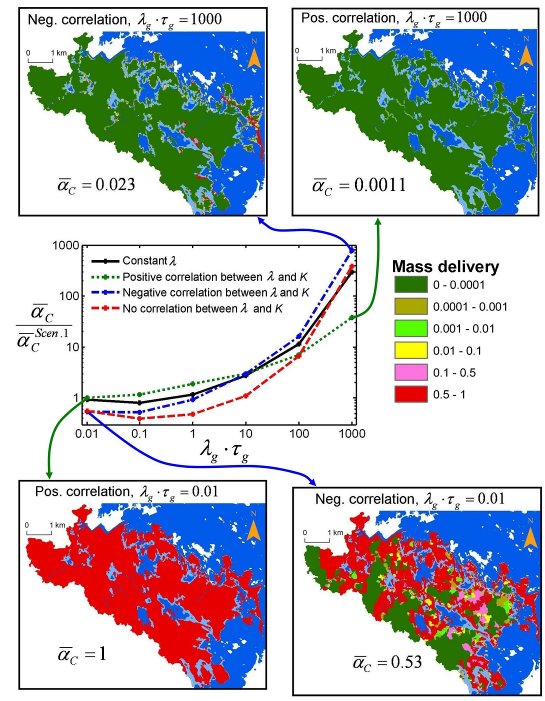


**Fig. 4.** The graph shows, for different assumptions regarding the correlation between $K$ and $\lambda$ in the $K$ variability scenario 2, the total (catchment-average) mass delivery fraction to the nearest surface water from all upstream input locations in the Forsmark catchment, $\bar{\alpha}_C$, relative to $\bar{\alpha}_C$ for the $K$ variability scenario 1 (in which both $K$ and $\lambda$ are constant). The maps exemplify the spatial distribution of the fraction of mass input that reaches the nearest surface water from all input locations within the catchment.




Discussion Paper | Discussion Paper | Discussion Paper | Discussion Paper |